

Refined TMD Gluon Density in a Proton from the HERA and LHC Data

A. V. Lipatov^{a,b,*}, G. I. Lykasov^b, and M. A. Malyshev^{a,c}

^aSkobeltsyn Institute of Nuclear Physics, Moscow State University, Moscow, 119991 Russia

^bJoint Institute for Nuclear Research, Dubna, Moscow region, 141980 Russia

^cMoscow Aviation Institute (National Research University), Moscow, 125993 Russia

*e-mail: lipatov@theory.sinp.msu.ru

Received April 15, 2024; revised April 26, 2024; accepted April 26, 2024

We update the phenomenological parameters of the Transverse Momentum Dependent (TMD, or unintegrated) gluon density in a proton proposed in our previous studies. This analysis is based on the analytical expression for starting gluon distribution which provides a self-consistent simultaneous description of HERA data on proton structure function $F_2(x, Q^2)$, reduced cross section for the electron-proton deep inelastic scattering at low Q^2 and soft hadron production in pp collisions at the LHC conditions. We extend it to the whole kinematical region using the Catani–Ciafaloni–Fiorani–Marchesini (CCFM) evolution equation. Exploiting our previous results on a number of semihard QCD processes, we performed a combined fit to an extended set of LHC and HERA data, comprising a total of 509 points from 16 data sets. We illustrate our fit by applying the derived TMD gluon density in a proton to inclusive prompt photon photoproduction at HERA.

DOI: 10.1134/S0021364024601234

It is well known that parton distribution functions in a proton (PDFs), $f_a(x, \mu^2)$ with $a = q$ or g , are an essential ingredient of any description of hard scattering at modern colliders energies. If only one scale is present in the process, $\mu \sim \sqrt{s} \gg \Lambda_{\text{QCD}}$, then the PDFs can be described in Quantum Chromodynamics (QCD) via the Dokshitzer–Gribov–Lipatov–Altarelli–Parisi (DGLAP) equations [1–4]. However, in case of a two-scale process, $\sqrt{s} \gg \mu \gg \Lambda_{\text{QCD}}$, the gluon dynamics can be described by the Balitsky–Fadin–Kuraev–Lipatov (BFKL) [5–7] or Catani–Ciafaloni–Fiorani–Marchesini (CCFM) [8–11] equations. It leads to Transverse Momentum Dependent (TMD, or unintegrated) gluon densities in a proton and high energy factorization [12, 13], or k_T -factorization [14, 15] approach (see review [16] for more information). The k_T -factorization approach is quite widely used in phenomenological applications and implemented in several Monte Carlo event generators, such as pegasus [17] and cascade [18]. A comprehensive set of TMD gluon distributions in a proton is available in the TMDLIB library [19].

In general, TMD gluon densities can be calculated within some approaches, such as popular Kimber–Martin–Ryskin formalism [20–22], Parton Branching approach [23, 24] or obtained from the analytical

or numerical solutions of BFKL-like QCD evolution equations. There are also investigations within the nonlinear (BK–JIMWLK) evolution in QCD (see, for example, [25–34] and references therein). The CCFM equation, which resumes large logarithmic terms proportional to $\alpha_s^n \ln^n 1/x$ and $\alpha_s^n \ln^n 1/(1-x)$ and therefore valid at both low and large x , has been applied [35]. In these calculations, the empirical expression for initial gluon density at some starting scale μ_0 (which is of the order of the hadron scale) with factorized Gauss smearing in transverse momentum was applied. In contrast, in our previous study [36] a more physically motivated expression for the input distribution was chosen. It is based on the description of the LHC data on soft hadron transverse momenta spectra in the framework of the modified soft quark gluon string model [37, 38] (see also [39–44]) with taking into account gluon saturation effects important at small x and scales of about the order of saturation scale Q_s [45]. The nonlinear effects in the subsequent QCD evolution were neglected (see discussion below). The obtained CCFM-evolved gluon density in a proton (LLM) was successfully tested later on a number of collider data, in particular, on latest HERA data on

longitudinal structure function of proton¹ $F_L(x, Q^2)$ [47] and associated photoproduction of prompt photons and jets [48].

Very recently it was shown [49] that some phenomenological parameters of the starting LLM gluon density need to be corrected in order to provide a good description (within the color dipole approach [48–53]) of the low Q^2 data on proton structure function $F_2(x, Q^2)$ and reduced deep inelastic cross sections taken by H1 and ZEUS Collaborations. These parameters are related mainly with the small x behavior of the TMD gluon density at low scales, as it will demonstrated below. Such corrections have been done already [49]. At the same time, this an adjustment does not spoil the quality of soft hadron spectra data, provided the corresponding parameters of fragmentation of quarks and diquarks to the hadrons are altered moderately (see [49] for more details). Of course, in this case essential parameters, which cannot be determined from these data, have to be fitted from other measurements with taking into account the effects connected with the QCD evolution of gluon density. It is the aim of this short work to perform such a fit using an extended set of experimental data for several processes known to be sensitive to the gluon content of the proton and then complete our study by applying the CCFM evolution to the newly fitted initial density. As a main result, we present a more universal TMD gluon distribution function in a proton, which is already available in the Monte Carlo event generator PEGASUS and TMDLIB tool.

So, we ended up with the following form (non-factorized with respect to x and \mathbf{k}_T^2) of the initial LLM gluon density in a proton:

$$f_g(x, \mathbf{k}_T^2) = c_g (1-x)^{b_g} \sum_{n=1}^3 c_n [R_0(x) |\mathbf{k}_T|]^n \exp(-R_0(x) |\mathbf{k}_T|), \quad (1)$$

where

$$R_0^2(x) = \frac{1}{Q_0^2} \left(\frac{x}{x_0} \right)^\lambda, \quad b_g = b_g(0) + \frac{4C_A}{\beta_0} \ln \frac{\alpha_s(Q_0^2)}{\alpha_s(\mathbf{k}_T^2)}, \quad (2)$$

with $C_A = N_C$, $\beta_0 = 11 - 2N_f/3$ and $Q_0 = 2.2$ GeV.

Here b_g parameter is treated to be running at $\mathbf{k}_T^2 > Q_0^2$ only, whereas the fixed value $b_g = b_g(0)$ at $\mathbf{k}_T^2 \leq Q_0^2$ is used. Simultaneous best fit to the HERA data on reduced deep inelastic cross section $\sigma_r(x, Q^2)$ and proton structure function $F_2(x, Q^2)$ measured at low $Q^2 < 4.5$ GeV² and LHC data on charged hadron

¹ A comparison of LLM predictions on $F_L(x, Q^2)$ with other models can be found [46].

(pion and kaon) production at small transverse momenta p_T in the mid-rapidity region leads to $c_1 = 5$, $c_2 = 3$, $c_3 = 2$, $x_0 = 1.3 \times 10^{-11}$ and $\lambda = 0.22$ [49]. The experimental data on charged hadron production involved into the fit are compared with our predictions in Fig. 1 (left panel). One can see that good agreement is achieved in a wide range of energies. For a comparison we also show the results obtained within the popular GBW model [25, 53]. It was argued [49] that the latter gives a somewhat worse description of the data. Note that the saturation dynamics given by (1) has been already discussed [49] (see also [36]). In particular, the predicted saturation scale² Q_s is of about $Q_s \sim 0.8$ GeV at very low $x \sim 10^{-11}$. This means that the nonlinear effects in the subsequent QCD evolution are practically absent and could be safely neglected, as it is often done in the framework of k_T -factorization (high energy factorization) approach. Thus, we apply here the linear CCFM equation³ to describe the QCD evolution, as we did earlier. Our choice is motivated mainly by the fact that the latter smoothly interpolates between the small- x BFKL gluon dynamics and large- x DGLAP one and therefore provides a suitable phenomenological tool.

Our procedure to determine remaining parameters, $b_g(0)$ and c_g , follows then the investigation [36]. As usual, they are extracted by minimizing

$$\chi^2 = \sum_i \left[\frac{\mathcal{C}_i^{\text{data}} - \mathcal{C}_i^{\text{theory}}}{\Delta \mathcal{C}_i^{\text{data}}} \right]^2, \quad (3)$$

where i runs over all experimental data points for observables \mathcal{C}_i from analyses listed in Table 1. Exploiting our previous results, theoretical predictions for each of \mathcal{C}_i are generated for large number of fixed guessed $b_g(0)$ values in the range $1 \leq b_g(0) \leq 9$ after applying the CCFM evolution to input density (1). At this step we used UPDFEVOLV routine [58] to solve numerically the CCFM equation. Note that the data set is extended now compared to the previous analysis [36] by including the ATLAS data [59] on inclusive b -jet production in pp collisions at $\sqrt{s} = 7$ TeV, CMS data on c -jet production in pp interactions at $\sqrt{s} = 2.76$ and 5.02 GeV [60] and HERA data [61, 62] on inclusive prompt photon photoproduction in ep collisions at $\sqrt{s} = 319$ GeV. Our simultaneous fit to all data sets leads to $b_g(0) = 5.109$ and $c_g = 1.2708$ with goodness $\chi^2/\text{d.o.f.} = 1.773$ for 509 data points, see

² The TMD gluon density does not depend on the scale at $\mu^2 < Q_s^2$.

³ Comprehensive numerical studies of the nonlinear JIMWLK equation were preformed. See, for example, [57] and references therein.

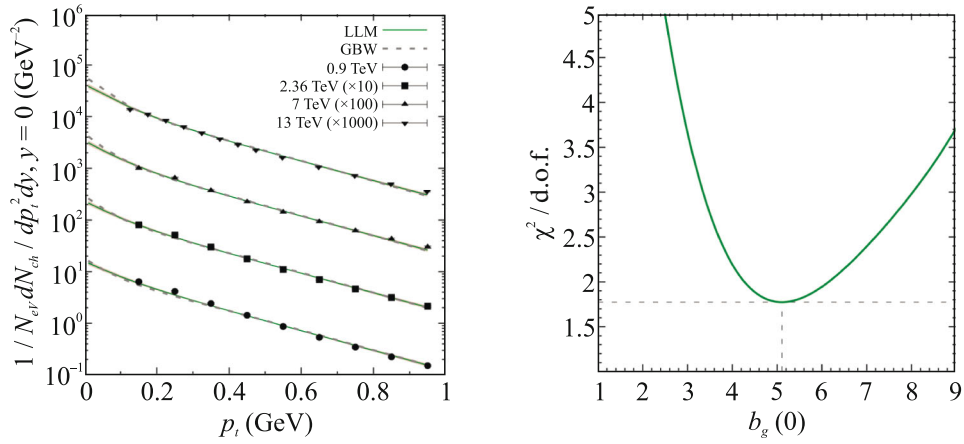


Fig. 1. (Color online) Left panel: transverse momentum distributions of multiplicities of soft charged hadrons produced in pp collisions at different LHC energies in the mid-rapidity region. Shaded bands correspond to the uncertainties of our calculations connected with the uncertainties in determination of x_0 and parton-to-hadron fragmentation parameters. The experimental data are from ATLAS [54, 55] and CMS [56]. Right panel: $\chi^2 / \text{d.o.f.}$ dependence of our fit for $b_g(0)$ parameter.

Fig. 1 (right panel). Then, to obtain the TMD gluon density in the whole kinematical range, we solved the CCFM equation numerically using the fitted values of the parameters above. In this way, the gluon distribution function (LLM) is tabulated in a commonly rec-

ognized format (namely, grid of $50 \times 50 \times 50$ bins in x , k_T^2 , and μ^2) which is used in the TMDLIB package. It is already available for public usage from there and implemented also into the Monte-Carlo event generator pegasus.

Table 1. List of experimental data used for the fitting procedure and number of data points for each experiment

| Experiment | Collaboration | Year | Reference | Collision | \sqrt{s}/GeV | Number of points |
|--|---------------|------------|-----------|------------------|-----------------------|------------------|
| Inclusive c -jet | CMS | 2017 | [60] | pp | 2.76 | 5 |
| Inclusive c -jet | CMS | 2017 | [60] | pp | 5.02 | 5 |
| Inclusive b -jet | ATLAS | 2011 | [59] | pp | 7 | 46 |
| Inclusive b -jet | CMS | 2012 | [63] | pp | 7 | 98 |
| $F_2^c(x, Q^2)$ | H1 | 2010, 2011 | [64, 65] | ep | 0.319 | 25 |
| $F_2^c(x, Q^2)$ | ZEUS | 2014 | [66] | ep | 0.319 | 18 |
| $F_2^b(x, Q^2)$ | H1 | 2014 | [64] | ep | 0.319 | 12 |
| $F_2^b(x, Q^2)$ | ZEUS | 2014 | [66] | ep | 0.319 | 17 |
| $\sigma_{\text{red}}^c(x, Q^2)$ | H1, ZEUS | 2018 | [67] | ep | 0.319 | 51 |
| $\sigma_{\text{red}}^b(x, Q^2)$ | H1, ZEUS | 2018 | [67] | ep | 0.319 | 27 |
| Inclusive $H \rightarrow \gamma\gamma$ | CMS | 2023 | [68] | pp | 13 | 37 |
| Inclusive $H \rightarrow \gamma\gamma$ | ATLAS | 2018 | [68] | pp | 13 | 27 |
| Inclusive $H \rightarrow ZZ^*$ | CMS | 2023 | [69] | pp | 13 | 54 |
| Inclusive $H \rightarrow ZZ^*$ | ATLAS | 2020 | [70] | pp | 13 | 54 |
| Inclusive γ | H1 | 2010 | [61] | ep , low Q^2 | 0.319 | 25 |
| Inclusive γ | ZEUS | 2014 | [62] | ep , low Q^2 | 0.319 | 8 |

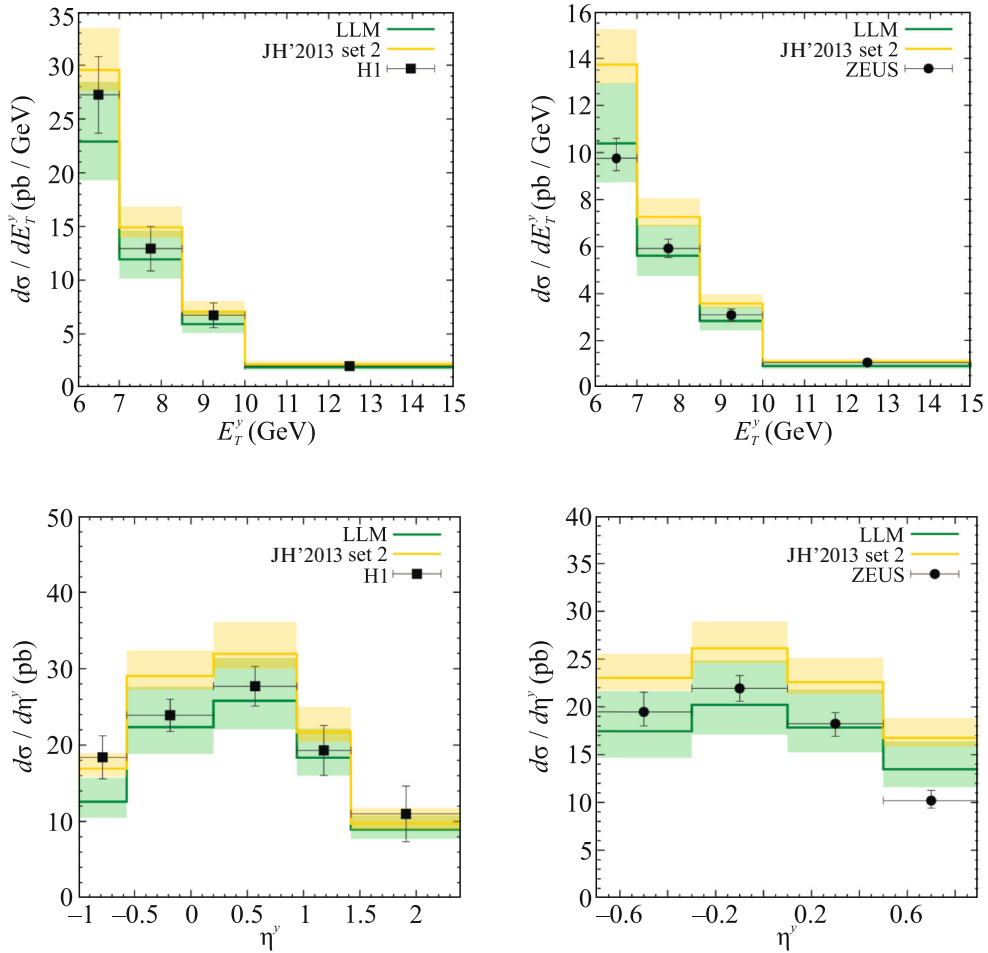


Fig. 2. (Color online) Inclusive prompt photon photoproduction cross section as a function of the photon transverse energy and pseudorapidity. The green (yellow) histograms and shaded bands correspond to the predictions obtained with the LLM (JH'2013 set 2) gluon density and estimated scale uncertainties of these calculations. The experimental data are from H1 [71] and ZEUS [72].

Let us now illustrate our fit with the inclusive prompt photon photoproduction in ep collisions at HERA, where sensitivity to the gluon density in a proton can be seen clearly. Here, in the photoproduction regime of DIS, the colliding electron emits a quasi-real photon, which then interacts with a proton. Here we completely follow our previous study [48], where we have investigated the prompt photon photoproduction with associated hadronic jets. The consideration is based on two leading off-shell (depending on the nonzero virtualities of incoming gluons) photon-gluon subprocesses, namely $\gamma g^* \rightarrow \gamma q\bar{q}$ and “box” subprocess $\gamma g^* \rightarrow \gamma g$, currently implemented into the Monte-Carlo event generator pegasus. The sea quark contribution is then incorporated in the former subprocess, while the small contribution of valence quarks can be taken into account in the conventional QCD factorization (see [48] for more details). Numerically, we use the massless limit for light (u , d , and s) quarks, set the charm and beauty masses to

$m_c = 1.4$ GeV and $m_b = 4.78$ GeV and implement certain kinematical cut applied in the experimental analyses:⁴ $6 < E_T^{\gamma} < 15$ GeV, $-1.0 < \eta^{\gamma} < 2.4$, $0.1 < y < 0.7$ for H1 measurement [61] and $6 < E_T^{\gamma} < 15$ GeV, $-0.7 < \eta^{\gamma} < 0.9$ and $0.2 < y < 0.7$ for ZEUS [62] one, where y is the fraction of the electron energy transferred to the photon (inelasticity). Both these data were obtained with the electron energy $E_e = 27.6$ GeV and proton energy $E_p = 920$ GeV. Results of our calculations for produced photon transverse energy and pseudorapidity distributions are shown in Fig. 2. One can see that our predictions (represented by the green histograms) are consistent with the latest HERA data within the experimental and theoretical uncertainties. The latter are estimated in a traditional

⁴ All kinematic quantities are given in the laboratory frame with positive OZ axis directed as the proton beam.

way, by varying the renormalization scale⁵ around its default value $\mu_R = E_T^\gamma$ as $\mu_R \rightarrow \xi \mu_R$ with $\xi = 1/2$ or 2. In contrast with newly fitted LLM set, using the JH'2013 set 2 gluon derived previously [35] leads to systematic overestimation of the HERA data in most of the bins, that coincides with observations made earlier [47, 48]. As it was argued [36], better agreement achieved with the LLM distribution is a consequence of using a physically motivated expression (1) for the initial gluon density for subsequent CCFM evolution. Thus, our calculations demonstrate that considered HERA data could help to distinguish the different approaches to evaluate the TMD gluon density in a proton. Exact determination of the latter, of course, is important for experiments at future electron-proton or electron-ion colliders, such as NICA, LHeC, FCC-eh, EiC, and EiCC.

Finally we would like to summarize the search for the phenomenological parameters of the proposed TMD gluon density in a proton, which has been performed in two steps. First, some parameters of the starting gluon distribution, which are not sensitive to the QCD evolution, have been found [49]. We point out that the analytical expression for the input (1) provides a self-consistent simultaneous description of HERA data on the proton structure function $F_2(x, Q^2)$, reduced cross section for the electron-proton deep inelastic scattering at low Q^2 and soft hadron production in pp collisions at the LHC conditions. Second, in this work, we continue the determination of phenomenological parameters (namely, $b_g(0)$ and c_g) with taking into account the effects of QCD evolution. Our procedure was based on a fit to a number of LHC and HERA data for processes sensitive to the gluon content of a proton at scale $\mu > Q_s$. The resulting fit quality ($\chi^2/\text{d.o.f.} = 1.773$) shows that the obtained gluon density does not contradict experimental data. We illustrate it additionally with latest HERA data on inclusive prompt photon photoproduction. Our results together with the ones [49] represent a self-consistent approach for the TMD gluon density in a proton valid in a wide kinematical region. The updated LLM gluon density supersedes previous version and can be used in different phenomenological applications for pp , $p\bar{p}$, and ep processes at modern and future colliders. It is available now in the TMDLIB library and Monte Carlo event generator pegasus.

ACKNOWLEDGMENTS

We thank S.P. Baranov, A.A. Prokhorov, and H. Jung for their interest, important comments and remarks.

⁵ In the CCFM-based approach, the factorization scale μ_F is related with the evolution variable and therefore should not be varied. See [8–11, 35] for more details.

A.V. Lipatov is grateful to the School of Physics and Astronomy, Sun Yat-sen University (Zhuhai, China) for warm hospitality.

FUNDING

This work was supported by ongoing institutional funding. No additional grants to carry out or direct this particular research were obtained.

CONFLICT OF INTEREST

The authors of this work declare that they have no conflicts of interest.

OPEN ACCESS

This article is licensed under a Creative Commons Attribution 4.0 International License, which permits use, sharing, adaptation, distribution and reproduction in any medium or format, as long as you give appropriate credit to the original author(s) and the source, provide a link to the Creative Commons license, and indicate if changes were made. The images or other third party material in this article are included in the article's Creative Commons license, unless indicated otherwise in a credit line to the material. If material is not included in the article's Creative Commons license and your intended use is not permitted by statutory regulation or exceeds the permitted use, you will need to obtain permission directly from the copyright holder. To view a copy of this license, visit <http://creativecommons.org/licenses/by/4.0/>

REFERENCES

1. V. N. Gribov and L. N. Lipatov, Sov. J. Nucl. Phys. **15**, 438 (1972).
2. L. N. Lipatov, Sov. J. Nucl. Phys. **20**, 94 (1975).
3. G. Altarelli and G. Parisi, Nucl. Phys. B **126**, 298 (1977).
4. Yu. L. Dokshitzer, Sov. Phys. JETP **46**, 641 (1977).
5. E. A. Kuraev, L. N. Lipatov, and V. S. Fadin, Sov. Phys. JETP **44**, 443 (1976).
6. E. A. Kuraev, L. N. Lipatov, and V. S. Fadin, Sov. Phys. JETP **45**, 199 (1977).
7. I. I. Balitsky and L. N. Lipatov, Sov. J. Nucl. Phys. **28**, 822 (1978).
8. M. Ciafaloni, Nucl. Phys. B **296**, 49 (1988).
9. S. Catani, F. Fiorani, and G. Marchesini, Phys. Lett. B **234**, 339 (1990).
10. S. Catani, F. Fiorani, and G. Marchesini, Nucl. Phys. B **336**, 18 (1990).
11. G. Marchesini, Nucl. Phys. B **445**, 49 (1995).
12. S. Catani, M. Ciafaloni, and F. Hautmann, Nucl. Phys. B **366**, 135 (1991).
13. J. C. Collins and R. K. Ellis, Nucl. Phys. B **360**, 3 (1991).
14. L. V. Gribov, E. M. Levin, and M. G. Ryskin, Phys. Rep. **100**, 1 (1983).

15. E. M. Levin, M. G. Ryskin, Yu. M. Shabelsky, and A. G. Shuvaev, Sov. J. Nucl. Phys. **53**, 657 (1991).
16. R. Angeles-Martinez, A. Bacchetta, I. I. Balitsky, et al., Acta Phys. Polon. B **46**, 2501 (2015).
17. A. V. Lipatov, M. A. Malyshev, and S. P. Baranov, Eur. Phys. J. C **80**, 330 (2020).
18. H. Jung, S. P. Baranov, A. Bermudez Martinez, L. I. Estevez Banos, F. Guzman, F. Hautmann, A. Lelek, J. Lidrych, A. V. Lipatov, M. A. Malyshev, M. Men-dizabal, S. Taheri Monfared, A. M. van Kampen, Q. Wang, and H. Yang, Eur. Phys. J. C **81**, 425 (2021).
19. N. A. Abdulov, A. Bacchetta, S. P. Baranov, et al., Eur. Phys. J. C **81**, 752 (2021).
20. M. A. Kimber, A. D. Martin, and M. G. Ryskin, Phys. Rev. D **63**, 114027 (2001).
21. A. D. Martin, M. G. Ryskin, and G. Watt, Eur. Phys. J. C **31**, 73 (2003).
22. A. D. Martin, M. G. Ryskin, and G. Watt, Eur. Phys. J. C **66**, 163 (2010).
23. F. Hautmann, H. Jung, A. Lelek, V. Radescu, and R. Zlebcik, Phys. Lett. B **772**, 446 (2017).
24. F. Hautmann, H. Jung, A. Lelek, V. Radescu, and R. Zlebcik, J. High Energy Phys. **1801**, 070 (2018).
25. J. Jalilian-Marian, A. Kovner, A. Leonidov, and H. Weigert, Phys. Rev. D **59**, 014014 (1998).
26. J. Jalilian-Marian, A. Kovner, A. Leonidov, and H. Weigert, Phys. Rev. D **59**, 014015 (1998).
27. A. Kovner, J. G. Milhano, and H. Weigert, Phys. Rev. D **62**, 114005 (2000).
28. E. Iancu, A. Leonidov, and L. D. McLerran, Nucl. Phys. A **692**, 583 (2001).
29. H. Weigert, Nucl. Phys. A **703**, 823 (2002).
30. E. Ferreiro, E. Iancu, A. Leonidov, and L. McLerran, Nucl. Phys. A **703**, 489 (2002).
31. I. Balitsky, Nucl. Phys. B **463**, 99 (1996).
32. Y. V. Kovchegov, Phys. Rev. D **60**, 034008 (1999).
33. K. Kutak and J. Kwiecinski, Eur. Phys. J. C **29**, 521 (2003).
34. K. Kutak and S. Sapeta, Phys. Rev. D **86**, 094043 (2012).
35. F. Hautmann and H. Jung, Nucl. Phys. B **883**, 1 (2014).
36. A. V. Lipatov, G. I. Lykasov, and M. A. Malyshev, Phys. Rev. D **107**, 014022 (2023).
37. V. A. Bednyakov, G. I. Lykasov, and V. V. Lyubushkin, Europhys. Lett. **92**, 31001 (2010).
38. V. A. Bednyakov, A. A. Grinyuk, G. I. Lykasov, and M. Poghosyan, Int. J. Mod. Phys. A **27**, 1250042 (2012).
39. A. B. Kaidalov, Z. Phys. C **12**, 63 (1982).
40. A. B. Kaidalov, Surv. High Energy Phys. **13**, 265 (1999).
41. A. B. Kaidalov and O. I. Piskunova, Z. Phys. C **30**, 145 (1986).
42. G. I. Lykasov and M. N. Sergeenko, Z. Phys. C **52**, 635 (1991).
43. G. I. Lykasov and M. N. Sergeenko, Z. Phys. C **56**, 697 (1992).
44. G. I. Lykasov and M. N. Sergeenko, Z. Phys. C **70**, 455 (1996).
45. A. H. Mueller, Nucl. Phys. B **335**, 115 (1990).
46. G. R. Boroun, Eur. Phys. J. A **60**, 48 (2024).
47. A. V. Lipatov, G. I. Lykasov, and M. A. Malyshev, Phys. Lett. B **839**, 137780 (2023).
48. A. V. Lipatov and M. A. Malyshev, Phys. Rev. D **108**, 014025 (2023).
49. A. V. Lipatov, G. I. Lykasov, and M. A. Malyshev, Phys. Lett. B **848**, 138390 (2024).
50. N. Nikolaev and B. G. Zakharov, Z. Phys. C **49**, 607 (1990).
51. N. Nikolaev, E. P. Predazzi, and B. G. Zakharov, Phys. Lett. D **326**, 161 (1994).
52. K. Golec-Biernat and M. Wüsthoff, Phys. Rev. D **59**, 014017 (1998).
53. K. Golec-Biernat and M. Wüsthoff, Phys. Rev. D **60**, 114023 (1999).
54. ATLAS Collab., New J. Phys. **13**, 053033 (2011).
55. ATLAS Collab., Eur. Phys. J. C **76**, 502 (2016).
56. CMS Collab., Phys. Rev. Lett. **105**, 022002 (2010).
57. S. Cali, K. Cichy, P. Korcyl, P. Kotko, K. Kutak, and C. Marquet, Eur. Phys. J. C **81**, 663 (2021).
58. F. Hautmann, H. Jung, and S. Taheri Monfared, Eur. Phys. J. C **74**, 3082 (2014).
59. ATLAS Collab., Eur. Phys. J. C **71**, 1846 (2011).
60. CMS Collab., Phys. Lett. B **772**, 306 (2017).
61. H1 Collab., Eur. Phys. J. C **66**, 17 (2010).
62. ZEUS Collab., Phys. Lett. B **730**, 293 (2014).
63. CMS Collab., J. High Energy Phys. **1204**, 084 (2012).
64. H1 Collab., Eur. Phys. J. C **65**, 89 (2009).
65. H1 Collab., Eur. Phys. J. C **71**, 1769 (2011).
66. ZEUS Collab., J. High Energy Phys. **1409**, 127 (2014).
67. ZEUS and H1 Collab., Eur. Phys. J. C **78**, 473 (2018).
68. CMS Collab., J. High Energy Phys. **2307**, 091 (2023).
69. CMS Collab., J. High Energy Phys. **2308**, 40 (2023).
70. ATLAS Collab., Eur. Phys. J. C **80**, 941 (2020).
71. H1 Collab., Eur. Phys. J. C **66**, 17 (2010).
72. ZEUS Collab., Phys. Lett. B **730**, 293 (2014).

Publisher's Note. Pleiades Publishing remains neutral with regard to jurisdictional claims in published maps and institutional affiliations.